

## Precision Test of Mass-Ratio Variations with Lattice-Confined Ultracold Molecules

T. Zelevinsky,<sup>1,\*</sup> S. Kotochigova,<sup>2</sup> and Jun Ye<sup>1</sup>

<sup>1</sup>*JILA, National Institute of Standards and Technology and University of Colorado, Boulder, Colorado 80309-0440, USA*

<sup>2</sup>*Physics Department, Temple University, Philadelphia, Pennsylvania 19122-6082, USA*

(Received 13 August 2007; published 29 January 2008)

We propose a precision measurement of time variations of the proton-electron mass ratio using ultracold molecules in an optical lattice. Vibrational energy intervals are sensitive to changes of the mass ratio. In contrast to measurements that use hyperfine-interval-based atomic clocks, the scheme discussed here is model independent and does not require separation of time variations of different physical constants. The possibility of applying the zero-differential–Stark-shift optical lattice technique is explored to measure vibrational transitions at high accuracy.

DOI: [10.1103/PhysRevLett.100.043201](https://doi.org/10.1103/PhysRevLett.100.043201)

PACS numbers: 06.20.Jr, 34.50.–s, 34.80.Qb, 37.10.De

Ultracold molecules open new opportunities for precision measurements of possible variations of fundamental physical constants. The test of time variation of the proton-electron mass ratio  $\Delta\mu/\mu$  ( $\mu \equiv m_p/m_e$ , where  $m_p$  and  $m_e$  are the proton and electron masses) is particularly suitable, since molecules are bound by electronic interactions while ro-vibrations are dominated by nuclear dynamics. Recent proposals to search for  $\Delta\mu/\mu$  include detecting changes in the atomic scattering length near a Feshbach resonance [1] or using near degeneracies of molecular vibrational levels from two different electronic potentials to probe microwave frequency shifts arising from  $\Delta\mu/\mu$  [2,3]. In contrast, we propose a two-color (Raman) optical approach to directly determine vibrational energy spacings within a single electronic potential of ultracold dimers in an engineered optical lattice. Utilizing the entire molecular potential depth, by selecting two vibrational levels with maximally different sensitivities to  $\Delta\mu/\mu$ , enhances the precision.

For a given physical system, there is a proportionality relation between  $\Delta\mu/\mu$  and the corresponding fractional change in the transition frequency  $\Delta\nu/\nu$ ,

$$\frac{\Delta\mu}{\mu} = \kappa \frac{\Delta\nu}{\nu}. \quad (1)$$

In the case discussed here,  $\kappa$  is of order one and has a small potential-dependent uncertainty. The fractional uncertainty  $\delta\mu/\mu$  of the measurement of  $(\Delta\mu \pm \delta\mu)/\mu$  must be minimized. For a given frequency measurement uncertainty  $\delta\nu$ , from Eq. (1) we obtain

$$\frac{\delta\mu}{\mu} = \kappa \frac{\delta\nu}{\nu} = \frac{d\ln\mu}{d\ln\nu} \frac{\delta\nu}{\nu} = \left( \frac{d\nu}{d\ln\mu} \right)^{-1} \delta\nu. \quad (2)$$

The last step in Eq. (2) is motivated by the assumption that experimental limitations constrain  $\delta\nu$  rather than  $\delta\nu/\nu$ . Equation (2) indicates that the quantity  $(d\nu/d\ln\mu)$  must be maximized. In other words, we search for the energy gaps with the maximum absolute frequency shifts arising from a given fractional mass-ratio change. While a microwave measurement [2,3] could have a smaller  $\delta\nu$  than the optical

frequency-comb-based Raman approach, the latter maximizes sensitivity through the cumulative effect of the entire molecular potential depth. The all-optical approach is also expected to suppress systematic shifts as it can be done Doppler and recoil free in the tight confinement of an optical lattice. Moreover, we propose to utilize the least sensitive energy gap as the reference, thus eliminating the frequency drift of any intermediate clock used in the experiment.

Most diatomic molecules based on laser-cooled atoms have similar ground state potential depths, within a factor of  $\sim 5$  ( $d\nu/d\ln\mu$  is proportional to the same factor). The homonuclear dimers can lead to higher precision than the heteronuclear counterparts, since their radiatively long-lived vibrational levels are insensitive to blackbody radiation. For the  $\Delta\mu/\mu$  experiment we propose to use molecules based on even isotopes of alkaline-earth-metal-type atoms (e.g., Sr, Ca, Yb). The lack of electronic and nuclear spin in their electronic ground state is one of the most attractive features, since it leads to a single ground state potential rather than a hyperfine manifold. As shown in previous work [4], this allows reliable theoretical modeling and prediction of vibrational energies. Another important property of molecules based on two-electron atoms is accessibility of spin-triplet metastable states. The metastable states have large Franck-Condon factors (FCFs) with the ground state [4]. Together with the absence of hyperfine structure and the narrow natural linewidths of the spin-forbidden transitions, this ensures that very low laser intensities are needed for making and probing the molecules. Furthermore, the zero angular momentum guarantees an absence of magnetic structure in the electronic ground state, simplifying the preparation of the system and reducing systematic shifts. In this work we focus on Sr<sub>2</sub>, as Sr can be routinely laser cooled to  $\sim 1$   $\mu$ K and is the atom of choice for many frequency metrology and precision measurements [5–9].

For the  $\Delta\mu/\mu$  experiment, vibrationally excited Sr<sub>2</sub> in the electronic ground state will be produced via photoassociation in an optical lattice [4]. Raman spectroscopy aided by a femtosecond optical frequency comb will inter-

rogate the energy spacings between deeply bound vibrational levels and those closer to the dissociation limit. The FCFs between the electronic ground state  $X$  potential (dissociating to  $^1S_0 + ^1S_0$ ) and the metastable  $0_u^+$  potential (dissociating to  $^1S_0 + ^3P_1$ , with ungerade symmetry and the atomic angular momentum projection onto the molecular axis  $\Omega = 0$ ) are sufficiently favorable to enable Raman transitions between two vibration levels in the  $X$  state via  $0_u^+$  (see Fig. 1). The relative stability of the Raman lasers can be maintained to better than 0.1 Hz [10]. Since the  $X$  potential is 30 THz deep [11–13] and we assume a power-broadened linewidth of 10 Hz and a signal to noise ratio of 100, the fractional precision can approach  $\sim 5 \times 10^{-15}/\sqrt{\tau}$  in the test of  $\Delta\mu/\mu$ , where  $\tau$  is the averaging time in seconds. This requires referencing the comb to an optical frequency standard [6].

Other tests based on atomic frequency metrology constrain  $\Delta\mu/\mu$  to  $\sim 6 \times 10^{-15}/\text{year}$  [14], and the recent evaluation of astronomical  $\text{NH}_3$  spectra limits  $\Delta\mu/\mu$  to  $\sim 3 \times 10^{-16}/\text{year}$  [15]. The atom-based tests rely on theoretical interpretations such as the Schmidt model, since electronic and fine structure transitions do not directly depend on  $\mu$ , and hyperfine transitions simultaneously depend on  $\mu$  and  $\alpha$  (the fine structure constant). The  $\text{NH}_3$  result is based on molecular lines and is therefore less model dependent, but relies solely on cosmological observations. In addition, it disagrees with the  $\text{H}_2$ -based result relevant to the same cosmological age ( $10^{10}$  years)

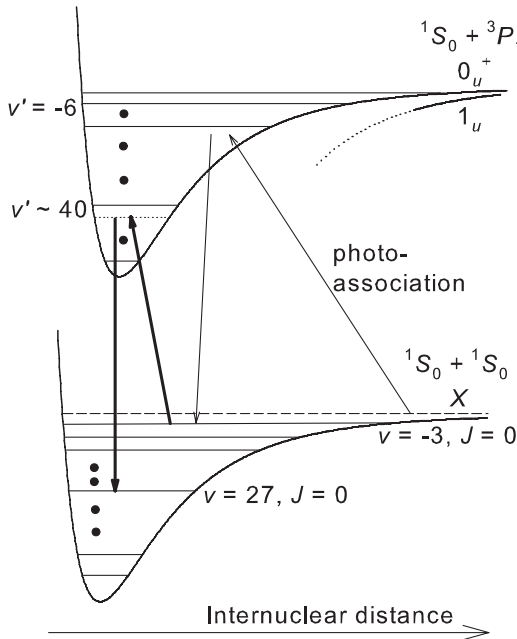


FIG. 1. A proposed scheme for precision Raman spectroscopy of  $\text{Sr}_2$  ground state vibrational level spacings. A two-color photoassociation pulse prepares molecules in the  $v = -3$  vibrational level. Subsequently, a Raman pulse couples  $v = -3$  and  $v = 27$ , via  $v' \sim 40$  of  $0_u^+$ . Negative vibrational numbers imply counting from the top of the potential with the least-bound level being  $-1$ .

that indicates nonzero  $\Delta\mu/\mu$  at the  $10^{-15}/\text{year}$  level [16]. The molecular system proposed here provides a direct test of present day variations with a competitive precision and a weak dependence on theoretical modeling [17].

In this work we select vibrational levels of the ground state potential [ $V(r)$ ] that have the largest and smallest sensitivities to  $\Delta\mu/\mu$ . To model  $V(r)$ , we combine the experimental  $\text{Sr}_2$  Rydberg-Klein-Rees potential [12] with its long-range dispersion form  $-C_6/r^6 - C_8/r^8$ , where  $C_6 = 3103(7) E_H a_B^6$  [18],  $C_8 = 1.9 \times 10^5 E_H a_B^8$  is determined by smoothly connecting to the Rydberg-Klein-Ree potential, and  $r$  is the internuclear separation in units of  $a_B$  ( $E_H = 4.36 \times 10^{-18}$  J and  $a_B = 0.0529$  nm). This model potential has 61 vibrational levels, depth  $D = 4.8 \times 10^{-3} E_H$ , the minimum at the internuclear separation  $r_0 = 8.4 a_B$ , and a scattering length of  $\sim 8 a_B$  [19,20]. A convenient approximation to the ground state potential is the Morse potential

$$V_M(r) = D(1 - e^{-a(r-r_0)})^2 - D, \quad (3)$$

where  $a \approx 0.7 a_B^{-1}$  for  $\text{Sr}_2$ . The Morse energy levels are

$$\epsilon_n = 2\epsilon_0(n + \frac{1}{2}) - \epsilon_0^2(n + \frac{1}{2})^2/D - D, \quad (4)$$

where  $\epsilon_0$  is approximately the zero-point energy. Note that the Morse spectrum is valid only if  $\epsilon_n - \epsilon_{n-1} > 0$ , or  $n < D/\epsilon_0$ , which means that  $V_M(r)$  has about  $N \sim 40$  bound levels. Figure 2(a) compares the  $\text{Sr}_2$  model potential and its Morse approximation.

Since  $\epsilon_0 \propto \mu^{-1/2}$ , the logarithmic derivative of the Morse expression for the  $n$ th vibrational energy level is

$$\frac{d\epsilon_n}{d\ln\mu} = -\epsilon_0(n + \frac{1}{2}) + \epsilon_0^2(n + \frac{1}{2})^2/D. \quad (5)$$

Equation (5) is the energy level sensitivity to a fractional mass-ratio change, with the highest absolute sensitivity for  $n_{\text{max}} \approx N/2$ , and the lowest sensitivity near the bottom and the top of the potential well. The sensitivities were also determined for the  $\text{Sr}_2$  model directly. Both the analytical Morse approximation and the more realistic calculation point to  $25 \lesssim v \lesssim 28$  as the most sensitive. Figure 2(b) shows the level sensitivities to  $\Delta\mu/\mu$ . We choose  $v = 27$  for the feasibility study, and the  $\Delta\mu/\mu$  measurement is optimized if either a weakly bound or the deepest vibrational level is chosen as the anchor level.

From considerations of sensitivity and transition strengths, we propose two complementary schemes for the measurement of  $\Delta\mu/\mu$ . The first scheme uses molecules in a highly excited vibrational level, while the second scheme adds a Raman step to drive the molecules into a deeper vibrational level. The difference of the two vibrational intervals, normalized by their sum, doubles the  $\Delta\mu/\mu$  sensitivity while eliminating any drift of a frequency reference used to stabilize the comb. Below, the rotational angular momenta are  $J = 0$  for  $X$  and  $J' = 1$  for  $0_u^+$  and  $1_u$ . The dipole moments for the relevant transitions were obtained using *ab initio* calculations [21].

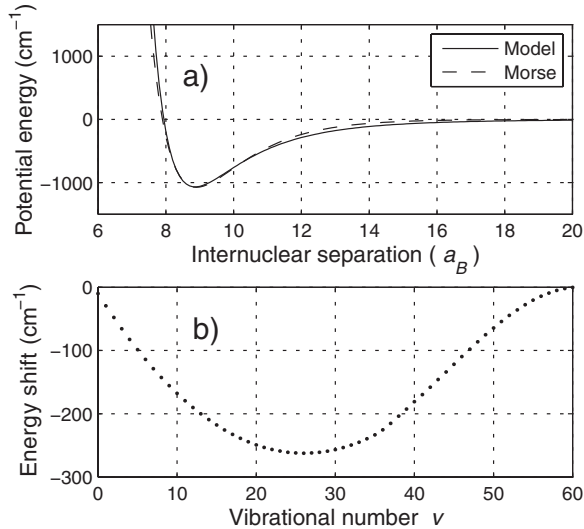


FIG. 2. (a) The model potential curve for the  $\text{Sr}_2$  ground state (solid line), and the Morse potential fitted to three parameters (dashed line). (b) Vibrational energy sensitivities to  $\Delta\mu/\mu$ , as a function of the vibrational number  $\nu$ .

Scheme I is illustrated in Fig. 1 and measures the energy difference between the weakly bound  $\nu = -3$  and  $\nu = 27$ , the latter being most sensitive to mass-ratio changes [see Fig. 2(b)]. Step Ia is two-color photoassociation into  $\nu = -3$  via  $\nu' = -6$  [4] using 689 nm light, with the two colors detuned by about 10 GHz (the primes refer to vibrational levels of the  $0_u^+$  excited electronic potential). Step Ib is three-level Raman spectroscopy,  $\nu = -3 \rightarrow \nu' \sim 40 \rightarrow \nu = 27$ . Figure 3 shows the transition dipole moments squared (DMS) that include FCFs and are defined as  $|\langle \nu, J | e\vec{r} | \nu', J' \rangle|^2$ , for  $\nu = 0$ ,  $\nu = 27$ , and  $\nu = -3$  to any vibrational level of  $0_u^+$ . For  $\nu = -3$  the DMS approach  $10^{-4} (ea_B)^2$  for a number of  $0_u^+$  vibrational levels with binding energies smaller than  $1000 \text{ cm}^{-1}$ , where  $e$  is the electron charge. For  $\nu = 27$  the maximum DMS are about hundredfold larger and quickly decrease for binding energies smaller than  $400 \text{ cm}^{-1}$ . This suggests using  $0_u^+$  intermediate levels with binding energies around  $400 \text{ cm}^{-1}$  to balance the Raman transition strengths, such that the laser wavelengths are in the 700–750 nm range. The resulting DMS of  $\sim 10^{-4} (ea_B)^2$  imply that for a 1 GHz detuning from the intermediate level  $\nu' \sim 40$  and laser intensities of  $2 \text{ W/cm}^2$ , the two-photon Rabi rate is  $\sim 2\pi \times 10 \text{ Hz}$ .

The complementary Scheme II probes deeper levels and includes an extra step of two-photon population transfer. Step IIa is identical to Ia. Step IIb is Raman population transfer  $\nu = -3 \rightarrow \nu' \sim 40 \rightarrow \nu = 27$ , analogous to Step Ib. Finally, Step IIc is  $\nu = 27 \rightarrow \nu' \sim 10 \rightarrow \nu = 0$  Raman spectroscopy (wavelengths  $\sim 700\text{--}800 \text{ nm}$ ). As shown in Fig. 3, the DMS between  $\nu = 0$  and the vibrational levels of  $0_u^+$  are very large near the bottom of  $0_u^+$  and decrease rapidly for levels with binding energies smaller than  $1500 \text{ cm}^{-1}$ . This suggests the choice of  $\nu' \sim 10$  for the intermediate level as it balances the DMS within the

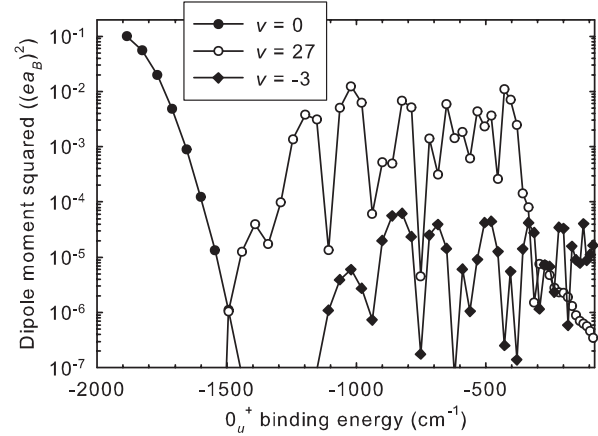


FIG. 3. Calculated dipole moments squared between vibrational levels of the  $X$  and  $0_u^+$  electronic states as a function of the binding energy for vibrational levels of  $0_u^+$  ( $J = 0$  and  $J' = 1$ ). The results for  $\nu = 0$ , 27, and  $-3$  of  $X$  are shown.

Raman transition to  $\sim 10^{-6} (ea_B)^2$ . For these transition strengths, and using 50 MHz detunings from  $\nu' \sim 10$  and Raman laser intensities of  $10 \text{ W/cm}^2$ , the Rabi rate for Step IIc is  $\sim 2\pi \times 10 \text{ Hz}$ .

The experiment critically depends on the control over systematic effects and the ability to perform Raman spectroscopy on a large number of molecules. Using an optical lattice trap is beneficial both for attaining high densities on the order of  $10^{12}/\text{cm}^3$  and for controlling systematic shifts [4]. The zero-differential-Stark-shift (or *magic frequency*) technique allows precise and accurate neutral-atom clocks [5–8,22]. It relies on the crossing of dynamic polarizabilities of the two probed states at a certain lattice frequency. Such a lattice ensures a vanishing differential Stark shift and a suppression of inhomogeneous Stark broadening. For photoassociation at the  $^1S_0 + ^3P_1$  dissociation limit, the polarization-dependent magic wavelength is near 914 nm ( $10950 \text{ cm}^{-1}$ ).

Analogously, we search for a zero-differential-Stark-shift lattice frequency for the proposed pairs of  $\text{Sr}_2$  vibrational levels of  $X$ . The Stark shifts of vibrational levels are proportional to dynamic polarizabilities [23] and are independent of the light polarization for  $J = 0$ . The polarizability of  $\text{Sr}_2$  in the vicinity of 914 nm slowly decreases with more weakly bound vibrational levels of  $X$ . However, by tuning the lattice frequency to near resonance with a vibrational transition from  $X$  to another excited electronic state  $1u$  we can match the polarizabilities of two vibrational levels in  $X$ . As shown in Fig. 4, our calculations reveal lattice frequency values in the vicinity of  $11000 \text{ cm}^{-1}$  for which the polarizabilities of  $\nu = 27$  and  $\nu = -3$ , as well as those of  $\nu = 0$  and  $\nu = 27$ , are equal. The precise location of the resonance depends on future experimental input.

A possible disadvantage of working near these resonances is enhanced scattering of lattice light. We estimate the scattering rate from the resonance strength as well as

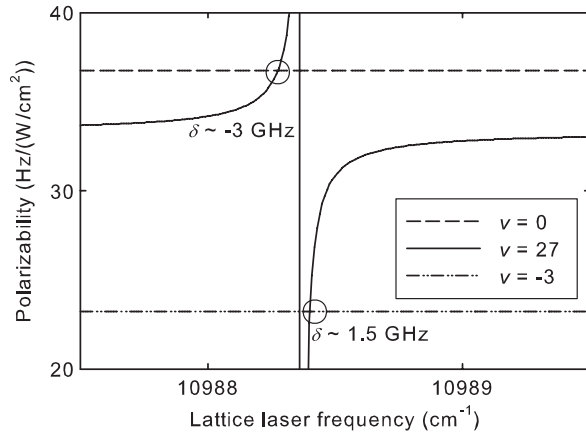


FIG. 4. Magic frequencies for the optical lattice near 910 nm ( $10990 \text{ cm}^{-1}$ ). The calculated detunings from resonance are  $\sim 1.5$  and  $-3$  GHz for Schemes I and II, respectively.

from the lattice detuning needed to achieve the zero-differential-Stark-shift condition. From our model, these detunings are  $\sim 1.5$  GHz for Scheme I and  $\sim -3$  GHz for Scheme II. Calculations show that the total spontaneous decay rate of  $1_u$  levels with  $4000 \text{ cm}^{-1}$  binding energy (as in Fig. 4) is  $2\pi\gamma = 2\pi \times 9 \text{ kHz}$ . The effective photon scattering rate is given by  $\Gamma_s \equiv 2\pi\gamma_s = (\pi s\gamma)/(2\delta/\gamma)^2$ , where  $\delta$  is the detuning from the resonance. The measure of the lattice intensity  $I$  is  $s$ , such that  $s = I/I_{\text{sat}}$ , with the effective saturation intensity for a single vibrational channel  $I_{\text{sat}} = (\pi c\hbar^2 \gamma^2)/(4f)$ , where  $2\pi\hbar$  is the Planck constant and  $f$  is the DMS [ $f \sim 5 \times 10^{-5} (e a_B)^2$  for the resonance in Fig. 4]. The estimated scattering rates are thus  $\sim 4/s$  for Scheme I and  $\sim 1/s$  for Scheme II, for  $I = 10 \text{ kW/cm}^2$ . This intensity supports a trap a few  $\mu\text{K}$  deep. Note that the scattering of lattice photons due to  $0_u^+$  vibrational levels, as well as nonresonant  $1_u$  levels, is strongly suppressed.

Further, we estimate the incoherent scattering rate of Raman lasers by the intermediate  $0_u^+$  levels. For the  $\nu = -3 \rightarrow \nu' \sim 40$  transition, this scattering rate is  $< 0.1/s$ , and for  $\nu = 27 \rightarrow \nu' \sim 10$ , the scattering rate is  $\sim 1/s$ , for Raman laser detunings and intensities given above. These estimates are conservative since the excited state population is expected to be suppressed when the Raman condition is fulfilled. Thus the scattering rates of the lattice and spectroscopy lasers will not limit the  $\sim 10$  Hz power-broadened linewidth of the two-photon transition.

The Stark shift of  $\nu$  due to one of the Raman lasers is  $\Delta = (s\gamma^2)/(8\delta) = \gamma_s(\delta/\gamma)$  in the large detuning limit. We estimate the near-resonant contributions to Stark shifts to be  $\sim 50$  Hz for both schemes for each Raman laser. Moreover, the shifts of the two vibrational levels within a Raman pair have the same sign which leads to cancellation with the proper power balance of the Raman beams. In addition to the near-resonant shift, there is a background shift due to other molecular levels (which can be partially compensated by slightly shifting the power balance in the

Raman beams). In the  $700\text{--}800 \text{ nm}$  wavelength range and for Raman laser intensities of  $\sim 10 \text{ W/cm}^2$ , the background Stark shifts are  $\sim 100$  Hz. Hence, in the worst case the Raman beam intensity must be controlled to  $< 0.1\%$  for inaccuracy  $< 0.1$  Hz.

Other major systematic effects are fluctuations of the magnetic field and atom density. Atomic clock work [5,6,24] demonstrates that they can be controlled to below  $0.1$  Hz, near the  $10^{-15}$  level, between subsequent measurements. Importantly, the absence of magnetic structure in the ground electronic state of  $\text{Sr}_2$  with  $J = 0$  should significantly suppress any magnetic shifts.

In conclusion, ultracold nonpolar molecules is an excellent system for measuring time variations of mass ratios, particularly if combined with a zero-differential-Stark-shift optical lattice designed for vibrational transitions. This system provides a self-referenced, model-independent test that is based on different physics than atomic clocks. We expect an initial test of  $\Delta\mu/\mu$  at  $\sim 10^{-15}/\text{year}$ , with a higher precision in the future.

We thank D. DeMille, P. Julienne, A. Derevianko, M. M. Boyd, and A. Ludlow for valuable discussions. We acknowledge NSF, NIST, DOE, and ARO for support.

\*Present address: Department of Physics, Columbia University, New York.

- [1] C. Chin and V. V. Flambaum, Phys. Rev. Lett. **96**, 230801 (2006).
- [2] D. DeMille *et al.*, this issue, Phys. Rev. Lett **100**, 043202 (2008).
- [3] V. V. Flambaum and M. G. Kozlov, Phys. Rev. Lett. **99**, 150801 (2007).
- [4] T. Zelevinsky *et al.*, Phys. Rev. Lett. **96**, 203201 (2006).
- [5] M. M. Boyd *et al.*, Phys. Rev. Lett. **98**, 083002 (2007).
- [6] A. D. Ludlow *et al.*, Science (to be published).
- [7] R. Le Targat *et al.*, Phys. Rev. Lett. **97**, 130801 (2006).
- [8] M. Takamoto *et al.*, J. Phys. Soc. Jpn. **75**, 104302 (2006).
- [9] G. Ferrari *et al.*, Phys. Rev. Lett. **97**, 060402 (2006).
- [10] A. D. Ludlow *et al.*, Opt. Lett. **32**, 641 (2007).
- [11] T. Bergeman *et al.*, J. Chem. Phys. **72**, 886 (1980).
- [12] G. Geber *et al.*, J. Chem. Phys. **81**, 1538 (1984).
- [13] E. Czuchaj *et al.*, Chem. Phys. Lett. **371**, 401 (2003).
- [14] S. G. Karshenboim *et al.*, arXiv:physics/0410074.
- [15] V. V. Flambaum and M. G. Kozlov, Phys. Rev. Lett. **98**, 240801 (2007).
- [16] E. Reinhold *et al.*, Phys. Rev. Lett. **96**, 151101 (2006).
- [17] Note that work by Chardonnet *et al.* on a beam of thermal  $\text{SF}_6$  molecules recently constrained the variation of the ratio of a vibrational frequency in  $\text{SF}_6$  to the Cs clock frequency to  $3 \times 10^{-14}/\text{year}$  (unpublished).
- [18] S. G. Porsev and A. Derevianko, JETP **102**, 195 (2006).
- [19] P. G. Mickelson *et al.*, Phys. Rev. Lett. **95**, 223002 (2005).
- [20] M. Yasuda *et al.*, Phys. Rev. A **73**, 011403(R) (2006).
- [21] S. Kotochigova, J. Chem. Phys. **128**, 024303 (2008).
- [22] H. Katori *et al.*, Phys. Rev. Lett. **91**, 173005 (2003).
- [23] S. Kotochigova and E. Tiesinga, Phys. Rev. A **73**, 041405(R) (2006).
- [24] T. Ido *et al.*, Phys. Rev. Lett. **94**, 153001 (2005).